Predicting Arrhythmias via Reentrant Vulnerability Index Mapping in Post-Infarction Hearts Under Stellate Ganglion Modulation

Javier Villar-Valero[1], Lledo Nebot[1], Juan F Gomez[2], David Soto-Iglesias[3], Giulio Falasconi[3], Antonio Berruezo[3], Bastiaan JD Boukens[4,5], Beatriz Trenor[1]

[1] Centro de Investigación e Innovación en Bioingeniería, Universitat Politècnica de València, Valencia, Spain
[2] Valencian International University, Valencia, Spain
[3] Arrhythmia Department, Heart Institute, Teknon Medical Center, Barcelona, Spain
[4] Department of Experimental Cardiology, Leiden University Medical Center, Leiden, Netherlands
[5] Department of Physiology, University Maastricht, Maastricht University Medical Center, Maastricht, The Netherlands

Abstract

Reentrant arrhythmias deriving from cardiac infarction scars can lead to sudden cardiac death. While implantable defibrillators are standard therapy, their limitations motivate alternative approaches such as autonomic modulation. This work sets computational ventricular models reconstructed from LGE-MRI data of two infarct cases, segmented into healthy tissue, border zone, and scar. Electrophysiological properties were assigned by tissue type, and sympathetic effects were modeled as IKs increases leading to ~30% APD shortening in stellate innervated regions. Programmed stimulation and Reentrant Vulnerability Index (RVI) analysis revealed that arrhythmia risk increased when sympathetic remodeling overlapped with the scar, whereas mismatched distributions had little effect. Sites of negative RVI values predicted reentry initiation, supporting RVI as a noninvasive marker of post-MI arrhythmic risk and a potential tool to guide autonomic modulation strategies.

1. Introduction

Sudden cardiac death following myocardial infarction (MI) remains one of the leading causes of mortality worldwide [1]. Most of these fatal events are due to reentrant ventricular arrhythmias developing on a vulnerable structural substrate, primarily infarct scars [2]. Implantable cardioverter defibrillators (ICDs) constitute the standard preventive therapy; however, they are associated with substantial limitations, including inappropriate shocks, mechanical complications, and adverse psychological effects [3].

In this context, modulation of the autonomic nervous system has emerged as an alternative therapeutic approach. In particular, sympathetic denervation through resection of the stellate ganglion (stellectomy) has been explored to reduce the incidence of arrhythmic events [4]. Nevertheless, its clinical efficacy varies, and significant side effects have been reported [5]. The ventricular electrophysiology is modulated by the left and right stellate ganglia, whose activity can be altered after MI [6]. This sympathetic remodeling contributes to a proarrhythmic environment, especially when combined with a vulnerable anatomical substrate and an appropriate trigger [7].

Despite growing interest in autonomic modulation, there are currently no non-invasive tools to identify which patients are most likely to benefit from these interventions or to determine which myocardial regions are more susceptible to reentrant activity. The present study addresses this gap by employing computational modeling to assess the interaction between post-infarction structural remodeling and sympathetic modulation. Specifically, we propose using the Reentrant Vulnerability Index (RVI) as a predictive biomarker to identify arrhythmogenic regions and stratify patient risk, providing a framework to guide and optimize autonomic therapies.

2. Methodology

2.1. Image Acquisition and Anatomical Reconstruction

We selected late gadolinium enhancement magnetic resonance imaging (LGE-MRI) datasets from two postinfarction patients. The methodology for image processing and anatomical reconstruction has been described in detail in our previous work (Villar-Valero et al., 2025) [8]; briefly,

we generated ventricular meshes from the LGEMRI data and segmented healthy myocardium, dense infarct core, and the surrounding border zone. Each mesh node was then labeled and coupled with the ventricular myocyte action potential model of O'Hara [9], with parameter adaptations for the different tissue types (healthy, scar, and border zone) as specified in our earlier study [8].

To simulate sympathetic modulation, we increased the conductance of the slow delayed rectifier potassium current (IKs) in the myocardial regions innervated by the stellate ganglion. We adjusted this conductance to achieve an action potential duration (APD) shortening of approximately 30%, in line with experimental evidence of sympathetic effects on ventricular electrophysiology [10].

2.2. Simulation Protocol

Simulations were performed using the ELVIRA solver for large-scale ventricular electrophysiology [11]. A stimulation protocol designed to mimic a clinical pacing maneuver was applied in order to investigate the arrhythmogenic substrate, following the methodology described in Villar-Valero et al. (2025) [8]. Six baseline stimuli (S1) at a basic cycle length (BCL) of 430 ms were delivered from the right ventricular apex. After these conditioning beats, a premature extra-stimulus (S2) was introduced with progressively shorter coupling intervals to test tissue vulnerability.

By pacing consistently from the right ventricular apex, a reproducible propagation pattern was ensured across the LV. This allowed an examination of how infarct-related conduction abnormalities, BZ remodeling, and sympathetic modulation interact when the tissue was subjected to premature stimulation. Whether these conditions could trigger functional reentry in the reconstructed ventricular models was investigated.

2.3. Calculation of the Reentrant Vulnerability Index

To quantify the susceptibility of the ventricular tissue to reentry, RVI was calculated, as initially proposed by Coronel et al. [12]. The RVI measures the temporal interplay between repolarization in a proximal region and activation in a distal region. When a propagating wavefront encounters tissue that is still refractory, conduction block occurs. However, if the wavefront bypasses the line of block and encounters tissue that has already repolarized, it can reenter the original site from the distal side. Whether reentry occurs depends on the time interval between proximal repolarization and distal activation times [13].

We defined the RVI between two sites i and j as:

$$\mathrm{RVI(i,j)} = \mathrm{RT(i)} - \mathrm{AT(j)}$$

Where RT(i) is the repolarization time at site i and AT(j) is the activation time at site j, computed within a neighborhood of radius 8 nodes. Negative RVI values indicate that the distal site is activated before the proximal site repolarizes, creating favorable conditions for reentrant initiation.

RVI maps were computed over all the ventricular geometries, particularly in regions near the BZ. Sympathetic stimulation resulted in shortened APD in selected areas, leading to local differences in repolarization timing. As a result, ganglion stellate innervated zones near the BZ could repolarize earlier than their surroundings. When a premature stimulus was applied under these conditions, such regions became potential reentry sites, as reflected by locally negative RVI values.

3. Results

3.1. Induction of Ventricular Arrhythmias

Our simulations revealed a higher inducibility of ventricular arrhythmias when sympathetic remodeling overlapped spatially with the infarcted region. Figure1 illustrates representative examples of the reentrant dynamics. Each panel shows a sequence of snapshots after delivery of the premature extra-stimulus, with times expressed as milliseconds after the S2 beat.

In Patient 1 (Figure 1A), we observed a clear difference between the two conditions. With stellate ganglion remodeling (upper row), the premature stimulus propagated throughout the ventricle, and after a short delay, a reentrant wavefront emerged. This wavefront reactivated the entire myocardium and initiated a sustained reentrant. In contrast, without stellate remodeling (lower row), the same premature stimulus failed to activate the ventricle, since the apex was still refractory at delivery. As a result, the stimulus did not propagate, and no arrhythmia was induced.

The behavior in Patient 2 (Figure 1B) was more subtle. The premature stimulus successfully captured the ventricle in both conditions—with and without stellate remodeling. The reduced APD associated with sympathetic activation was insufficient to alter refractoriness at the stimulation site. However, the outcome diverged after full ventricular activation: with stellate remodeling (upper row), the extra-stimulus gave rise to a reentrant wavefront that re-excited the myocardium and initiated sustained arrhythmia. In contrast, without remodeling (lower row), the activation propagated but eventually extinguished. Only isolated regions of delayed activation persisted, without forming a closed pathway capable of supporting reentry.

These results show that the presence of stellate remodeling not only alters global APD distributions but also facilitates reentry initiation when premature beats are delivered in the context of scar and border zone heterogeneities.

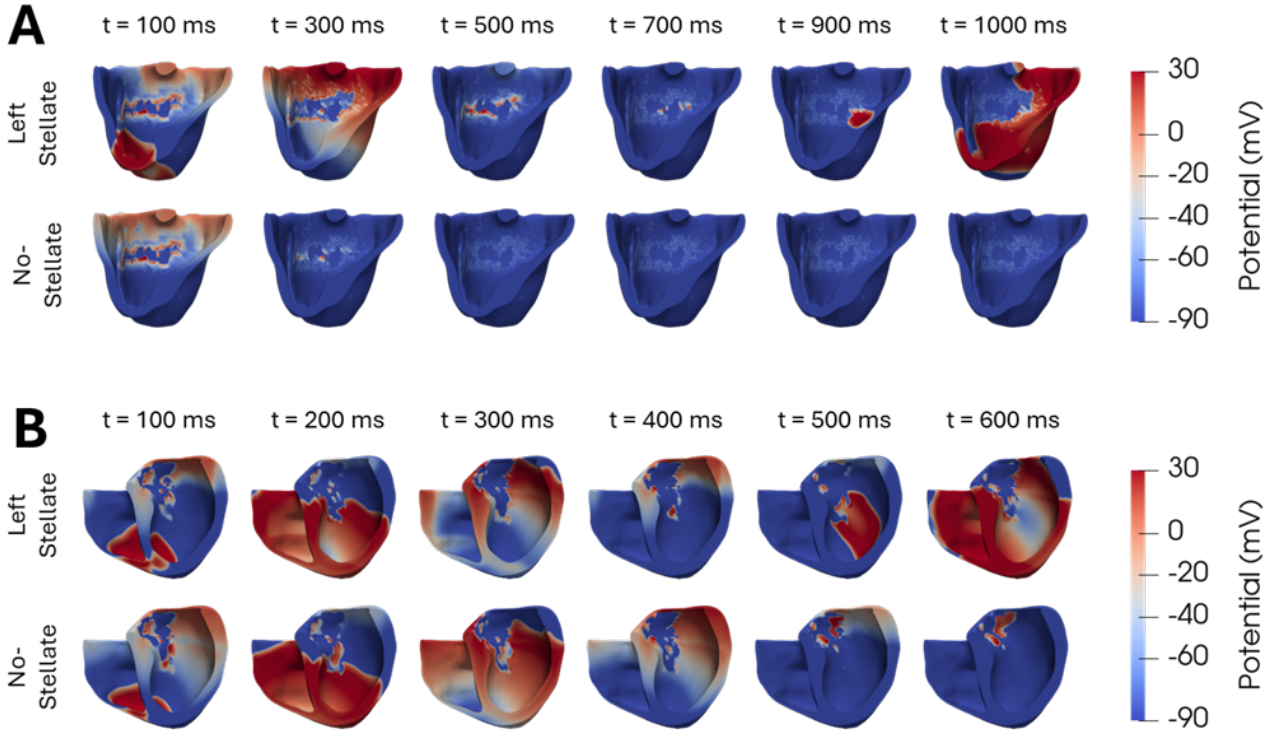

Figure 1. Spatiotemporal activation maps from two post-infarction patients following delivery of a premature extra-stimulus. Panel A corresponds to Patient 1 (anterior infarction) and Panel B to Patient 2 (posterior infarction). For each patient, the upper row shows the simulation with left stellate ganglion remodeling, while the lower row shows the simulation without stellate ganglion remodeling. Numbers indicate the time in milliseconds elapsed after the premature extra-stimulus.

3.2. RVI Mapping and Prediction of Reentrant Sites

RVI maps were computed in both geometries to further investigate the mechanisms underlying these differences. For the simulations that led to sustained reentry (both cases with stellate remodeling), localized regions of highly negative RVI values were found. These regions spatially overlapped with the sites where reentrant wavefronts subsequently emerged.

Figure 2 illustrates this relationship. On the left side of each panel, we show the RVI distribution computed immediately after the last basic stimulus (before delivery of the premature beat). A snapshot from the arrhythmia inducing simulation is displayed on the right side, highlighting the reentrant wavefront as it exits its point of origin to reactivate the ventricle.

We observed a qualitative and spatial correlation between the most negative RVI regions and the actual reentry sites. This suggests that the index can identify vulnerable areas even before premature stimulation triggers an arrhythmia. Notably, this predictive pattern emerged even when we calculated RVI after a single pacing sequence, without requiring the complete clinical induction protocol.

4. Discussion

Our results highlight the differential role of sympathetic modulation based on the specific stellate ganglion affected and the location of the infarct. We introduced heterogeneity in APD distributions across the ventricle, Figure 1. Spatiotemporal activation maps from two post-infarction patients following delivery of a premature extra-stimulus. Panel A corresponds to Patient 1 (anterior infarction) and Panel B to Patient 2 (posterior infarction). For each patient, the upper row shows the simulation with left stellate ganglion remodeling, while the lower row shows the simulation without stellate ganglion remodeling.

Especially in areas controlled by the left stellate ganglion, a dispersion of repolarization could facilitate reentry. We found that arrhythmic risk increases markedly when the territory innervated by the stellate ganglion overlaps with the infarct scar, whereas mismatched remodeling had minimal effect. This observation supports the need for patient-specific approaches in autonomic denervation therapies and is consistent with clinical studies reporting vari-

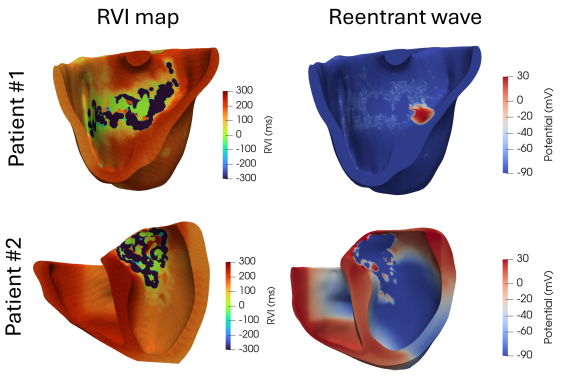

Figure 2. RVI maps and reentrant wavefront initiation in two post-infarction patients. First column: RVI distribution after the last basic stimulus. Second column: snapshot of arrhythmia simulation at reentrant wavefront emergence. Rows: Patient 1 (top), Patient 2 (bottom).

ability in the efficacy of stellectomy across patients [4].

In addition, we propose that the RVI, when integrated with personalized anatomical and electrophysiological modeling, can identify arrhythmogenic regions in a noninvasive manner. By anticipating reentry-prone sites without requiring aggressive stimulation protocols, RVI mapping could provide clinically relevant insights for post-MI risk stratification and guiding autonomic therapeutic strategies.

5. Conclusion

This article indicates that sympathetic remodeling after myocardial infarction, mediated by the stellate ganglia, may modulate the risk of reentrant arrhythmias location-dependent. The RVI appears to identify regions prone to reentry without requiring invasive stimulation protocols. Integrating patient-specific computational modeling with predictive biomarkers such as RVI points to a promising strategy for optimizing antiarrhythmic therapies in post-MI patients.

Acknowledgments

This work was supported by Grant PRE2020-091849 [MCIN/AEI/10.13039/501100011033] and "ESF Investing in your future"; Grant PID2019 104356RB-C41 [MCIN/AEI/10.13039/501100011033]; PID2022- 136273OA-C33 and PID2022-140553OB-C41 [MICIU/AEI/ 10.13039/501100011033 and by ERDF/EU]; Barcelona Supercomputing Center, Spain [IM-2024-1-0010, IM-2024-2-0015, IM-2024-3-0001, IM-2025-1-0010 and IM-2025-2-0007]; and Teknon projects.

References

[1] World Health Organization. Cardiovascular Diseases, 2021. URL https://www.who.int/news-room/fact-sheets/detail/cardiovascular-diseases-(cvds).

[2] Willems AR, Tijssen JG, van Capelle FJ, Kingma JH, Hauer RN, Vermeulen FE, Brugada P, van Hoogenhuyze DC, Janse MJ. Determinants of prognosis in symptomatic ventricular tachycardia or ventricular fibrillation late after myocardial infarction. Journal of the American College of Cardiology 1990;16(3):521–530. ISSN 07351097.

[3] Olde Nordkamp LR, Wilde AA, Tijssen JG, Knops RE, Van Dessel PF, De Groot JR. The ICD for primary prevention in patients with inherited cardiac diseases: Indications, use, and outcome: A comparison with secondary prevention. Circulation Arrhythmia and Electrophysiology feb 2013;6(1):91–100. ISSN 19413149.

[4] Vaseghi M, Barwad P, Malavassi Corrales FJ, Tandri H, Mathuria N, Shah R, Sorg JM, Gima J, Mandal K, Sàenz Morales LC, Lokhandwala Y, Shivkumar K. Cardiac sympathetic denervation for refractory ventricular arrhythmias. Journal of the American College of Cardiology June 2017;69(25):3070–3080. ISSN 1558-3597.

[5] Herring N, Kalla M, Paterson DJ. The autonomic nervous system and cardiac arrhythmias: current concepts and emerging therapies. Nature Reviews Cardiology dec 2019;16(12):707–726. ISSN 17595010.

[6] Gardner RT, Ripplinger CM, Myles RC, Habecker BA. Molecular mechanisms of sympathetic remodeling and arrhythmias. Circulation Arrhythmia and Electrophysiology February 2016;9(2). ISSN 1941-3084.

[7] Waddell-Smith KE, Ertresvaag KN, Li J, Chaudhuri K, Crawford JR, Hamill JK, Haydock D, Skinner JR. Physical and psychological consequences of left cardiac sympathetic denervation in long-qt syndrome and catecholaminergic polymorphic ventricular tachycardia. Circulation Arrhythmia and Electrophysiology October 2015; 8(5):1151–1158. ISSN 1941-3084.

[8] Villar-Valero J, Gomez JF, Soto-Iglesias D, Penela D, Berruezo A, Trenor B. Computational modeling of post-myocardial infarction arrhythmias: Insights and predictions. Computers in Biology and Medicine sep 2025;196:110894. ISSN 0010-4825.

[9] O'Hara T, Virág L, Varró A, Rudy Y. Simulation of the undiseased human cardiac ventricular action potential: Model formulation and experimental validation. PLoS Computational Biology 2011;7(5). ISSN 1553734X.

[10] Meijborg VM, Boukens BJ, Janse MJ, Salavatian S, Dacey MJ, Yoshie K, Opthof T, Swid MA, Hoang JD, Hanna P, Ardell J, Shivkumar K, Coronel R. Stellate ganglion stimulation causes spatiotemporal changes in ventricular repolarization in pig. Heart Rhythm 2020;17(5):795–803. ISSN 15563871.

[11] Heidenreich EA, Ferrero JM, Doblaré M, Rodríguez JF. Adaptive macro finite elements for the numerical solution of monodomain equations in cardiac electrophysiology. Annals of Biomedical Engineering 2010;38(7):2331–2345. ISSN 00906964.

[12] Coronel R, Wilms-Schopman FJ, Opthof T, Janse MJ. Dispersion of repolarization and arrhythmogenesis. Heart Rhythm apr 2009; 6(4):537–543. ISSN 15475271.

[13] Campos FO, Orini M, Taggart P, Hanson B, Lambiase PD, Porter B, Rinaldi CA, Gill J, Bishop MJ. Characterizing the clinical implementation of a novel activation-repolarization metric to identify targets for catheter ablation of ventricular tachycardias using computational models. Computers in Biology and Medicine may 2019; 108:263–275. ISSN 0010-4825.

Address for correspondence:

Beatriz Trenor
Email: btrenor@eln.upv.es
Centro de Investigación e innovación en Bioingenieria (Ci2B), Universitat Politècnica de València (UPV)
Camino de Vera s/n, 46022. Valencia, Spain.